Department of Pharmaceutics[1], School of Pharmacy, Guangdong Pharmaceutical University; Department of Pharmacy[2], Guangdong Provincial People's Hospital, Guangdong Academy of Medical Sciences, Guangzhou, China

Design and development of functionalized single-walled carbon nanotube-ethosomes for transdermal delivery of ketoprofen

J. Xiaowei[1], Y. Lijuan[1], L. Yanling[1], L. Qiuxiao[2], G. Bohong[1,*]

Received December 6, 2022, accepted February 9, 2023

**Corresponding author: Bohong Guo, Department of Pharmaceutics, School of Pharmacy, Guangdong Pharmaceutical University, 280 East Waihuan Road, Guangzhou Higher Education Mega Center, Guangzhou, 510006, China guobohong@gdpu.edu.cn*

Pharmazie 78: 31-36 (2023) *doi: 10.1691/ph.2023.2572*

The purpose of this study was to combine carbon nanotube with ethosomes in order to obtain hybrid nanocarriers for transdermal delivery of ketoprofen (KP). KP-loaded functionalized single-walled carbon nanotube (f-SWCNTs) composite ethosomes (f-SWCNTs-KP-ES) were designed and were verified by a series of characterizations. The particle size of the preparation is less than 400 nm. DSC and XRD experiments showed that KP existed in an amorphous state after it was adsorbed and loaded on f-SWCNTs. TEM experiments showed that the structure of SWCNTs remained intact after oxidation and modification by PEI. FTIR results showed that PEI were successfully modified on the surface of SWCNT-COOH, and KP was successfully loaded on f-SWCNTs. *In vitro* release characteristics showed that the preparation had sustained release behavior and conformed to the first-order kinetic equation model. In addition, f-SWCNTs-KP-ES gel were prepared and *in vitro* skin permeation and *in vivo* pharmacokinetics were studied. The results showed that f-SWCNTs-KP-ES gel could enhance the skin permeation rate of KP and increase the drug retention of drugs in the skin. The characterization results consistently showed f-SWCNTs is a promising drug carrier. The hybrid nanocarrier prepared by the combination of f-SWCNTs and ethosomes can enhance the transdermal absorption of drugs and improve the bioavailability of drugs, which has a certain significance for the development of advanced hybrid nano-preparations.

1. Introduction

The main barrier of transdermal drug delivery is the stratum corneum. Transdermal drug delivery system affects cell uptake of drugs, drug efficacy and adverse drug reactions, etc. The research and development of a new drug delivery system is of great significance to enhance the transdermal delivery, increase the uptake rate by cells and improve the efficacy of drugs.

In recent years, carbon nanotubes (CNTs) have attracted research interest because of their excellent aspect ratio, cell absorption efficiency and convenient transmembrane transport, and have been especially used in pharmaceutical and medical fields as a drug delivery system (Hua et al. 2013). The structure of CNTs enhances the direct absorption through the cell membrane without any detrimental effect on the biological function of the cell. But the dosage of CNTs loaded drugs is limited, and the water solubility of CNTs is low. The toxicology of CNTs remains undetermined and longer carbon nanotubes are more cytotoxic, which limits the application of CNTs. Therefore, the functionalization of CNTs can shorten the carbon chain, increase water solubility and optimize the function of CNTs. In addition, liposomes are widely used in drug delivery systems because of their excellent drug loading, biocompatibility and biodegradability. Therefore, CNTs and liposomes are covalently combined to prepare a CNTs-liposome drug delivery platform, which realizes the combination of high uptake rate and high drug loading, which is of great significance for the development of advanced drug delivery system.

Compared with liposomes, ethosomes have shown greater success in increasing the amount and depth of skin penetration of many drugs (Paolino et al. 2005; Zhai et al. 2015; Nainwal et al. 2019). Ethosomes have good elasticity and can pass through the stratum corneum into the deep layers of the skin, thus increasing the penetration of drugs. Therefore, the purpose of this study was to combine CNTs with ethosomes in order to obtain hybrid nanocarriers for transdermal delivery of drugs, so as to improve the bioavailability of drugs and prolong the retention time of drugs. KP was chosen as the model drug for transdermal delivery. But the poor stability, low solubility and adverse reactions such as gastrointestinal ulcer and bleeding after oral administration has affected the clinical application of KP (Manikkath et al. 2017; Jyothsna et al. 2017; Hegde et al. 2017). Therefore, in recent years, many studies have been carried out on the drug delivery forms of KP, such as ethosomes, inclusion complexes, controlled release, sustained release and so on, in order to improve the bioavailability of the drug and reduce the toxicity and side effects (Malinovskaja-Gomez et al. 2017; Xing and Lu 2018). Transdermal delivery of KP can reduce adverse reactions, improve the bioavailability and prolong the sustained release (Kurniawan et al. 2019; Kaleemullah et al. 2017).

Based on the above, we prepared f-SWCNTs and investigated the water dispersibility of functionalized carbon nanotubes. We designed KP-loaded f-SWCNTs composite ethosomes (f-SWCNTs-KP-ES) and the preparation was characterized by particle size potential measurement, DSC, XRD, TEM observation

Abbreviations
SWCNTs=single-walled carbon nanotubes; p-SWCNTs=pristine single-walled carbon nanotubes; f-SWCNTs=functionalized single-walled carbon nanotubes; f-SWCNTs-KP=ketoprofen-loaded functionalized single-walled carbon nanotubes; f-SWCNTs-KP-ES=ketoprofen-loaded functionalized single-walled carbon nanotubes composite ethosomes; KP=ketoprofen; KP-ES=ketoprofen ethosomes; TEM=transmission electron microscopy; DSC=differential scanning calorimetry; XRD=X-ray diffraction; FTIR=fourier transform infrared; PBS= phosphate-buffered saline; RB= rhodamine B; SD=standard deviation.

and FTIR and *in vitro* release characteristics. For the prepared f-SWCNTs-KP-ES gel, Franz diffusion cell method was used to study *in vitro* skin permeation, and Rhodamine B (RB) fluorescence labeling was used to investigate the retention of KP in the skin and study *in vivo* pharmacokinetics.

2. Investigations, results and discussion

2.1. Water dispersibility of carbon nanotubes

Figure 1A shows, from left to right, the results of water dispersibility of p-SWCNTs, SWCNTs-COOH and f-SWCNTs. The p-SWCNTs were poorly dispersed and stratified precipitation occurred after ultrasonic placement. The water dispersibility of the SWCNTs-COOH was greatly improved because the length was truncated and carboxyl groups of water-soluble functional groups were connected during oxidation. However, large particles were still formed after placement, and obvious sediment was produced at the bottom of the bottle. The f-SWCNTs had good dispersion in distilled water, the whole system was a uniform black solution, and there was no stratified precipitation after several days, which is similar to Xie's study (Zhu et al. 2014). These illustrated that after strong acid oxidation of carbon nanotubes, the size of carbon nanotubes was significantly reduced, and the introduction of hydrophilic carboxyl and PEI further improved the water dispersibility and stability of carbon nanotubes.

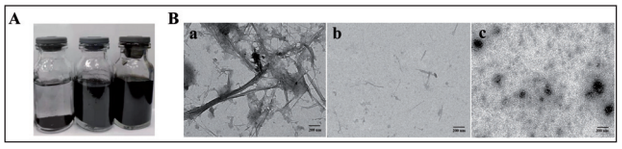

Fig. 1: (A) Water dispersibility of carbon nanotubes and (B) TEM images of SWCNTs system: (a): p-SWCNTs; (b): f-SWCNTs; (c): f-SWCNTs-KP-ES

2.2. Characterization of SWCNTs system

TEM images are shown in Fig. 1B. The p-SWCNTs were aggregated and wound into bundles, which could explain why they precipitated at the bottom of the vial when studying the water dispersion of carbon nanotubes. The size of SWCNTs became shorter after strong acid oxidation, but the structure remained basically intact (Farahani et al. 2015). Some researchers found that with the increase of oxidation time, the more the structure of carbon nanotubes is destroyed, and when the oxidation time is more than six hours, the structure of carbon nanotubes will be seriously damaged and a large number of fragments will be produced (Mishra et al. 2018). In this experiment, the oxidation time was three hours, and the reaction conditions were suitable, so the structure of more complete carbon nanotubes could be obtained. As shown in Fig. 1C, the morphology of the f-SWCNTs-KP-ES hybrid nano-preparation can be seen clearly, which has a spherical structure. The structure should be ethosomes, which are surrounded by drug-loaded SWCNTs, and a small amount of SWCNTs are wound and interspersed on the outside (Miyako et al. 2012). TEM image showed that the particle sizes of f-SWCNTs and f-SWCNTs-KP-ES were in the range of 200-400 nm, corresponding to subsequent particle sizes measurements.

The results of particle size and Zeta potential are shown in Fig. 2. The average particle sizes of KP-ES, f-SWCNTs, f-SWCNTs-KP and f-SWCNTs-KP-ES were 129.0±1.00 nm, 192.29±8.14 nm, 264.00±5.19 nm and 388.26±4.99 nm, respectively, and the polymer polydispersity index (PDI) was less than 0.3 (Table 1). It can be seen from the data that the particle size of f-SWCNTs-KP was larger than that before drug loading, which may be due to the fact that a large number of drugs were adsorbed into the surface of SWCNTs. In addition, the particle size of the hybrid nanocarrier f-SWCNTs-KP-ES was the largest because it was a hybrid of f-SWCNTs-KP wrapped with ethosomes. It can be seen from Table 1 that the Zeta potentials of KP-ES and f-SWCNTs-KP were -13.43±1.81 and 16.71±1.31, respectively, while the Zeta potentials of f-SWCNTs-KP-ES was close to zero, which indicated that f-SWCNTs-KP could effectively bind to the bi-layer structure of ethosomes (Zhu et al. 2014).

Table 1: The particle size, PDI and Zeta potential of nano-preparations

Formulations	Particle size (nm)	PDI	Zeta potential (mV)
KP-ES	129.00±1.00	0.262±0.010	-13.43±1.81
f-SWCNTs	192.29±8.14	0.232±0.023	13.00±0.02
f-SWCNTs-KP	264.00±5.19	0.286±0.012	16.71±1.31
f-SWCNTs-KP-ES	388.26±4.99	0.223±0.049	-3.94±1.51

Abbreviations: PDI: polydispersity index

DSC thermograms are shown in Fig. 3A. There was a strong diffraction peak at 95.0 °C, which should be the melting point of KP, and the blank carrier f-SWCNTs had no endothermic peak in the range of 30–280 °C, which did not interfere with the DSC analysis of drug-loaded preparations (Perpétuo et al. 2017). Meanwhile, there was no peak of f-SWCNTs-KP in the determination range, indicating that after being adsorbed and loaded on the f-SWCNTs, KP was no longer in crystalline state, but in amorphous or molecular state.

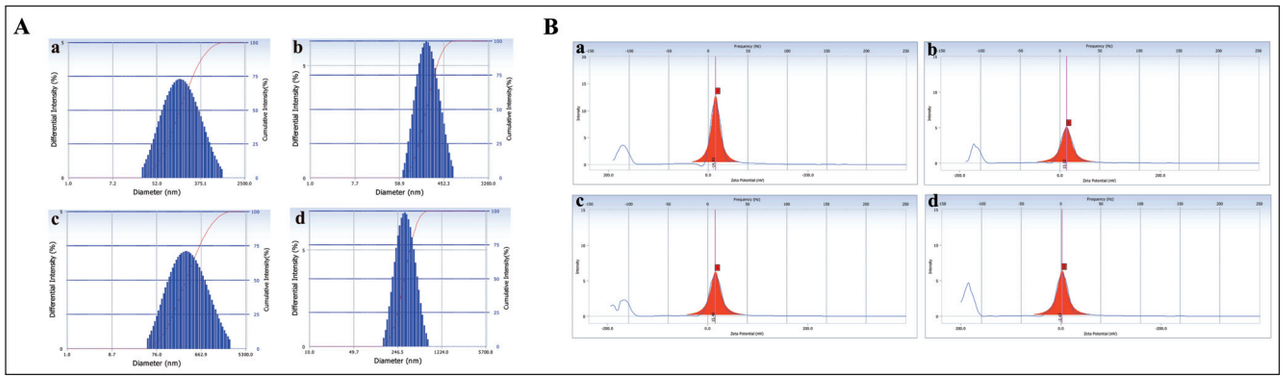

Fig. 2: (A) Particle size and (B) zeta potentials of (a): KP-ES; (b): f-SWCNTs; (c): f-SWCNTs-KP; (d): f-SWCNTs-KP-ES

XRD spectra are shown in Fig. 3B. Multiple diffraction peaks of pure KP were observed at 6.40°, 14.48°, 18.58°, 20.08°, 22.93° and 24.05°, indicating that KP was a high crystallization drug (Dantas de Freitas et al. 2018). Whereas, there was no characteristic peak of KP in relevant position for f-SWCNTs-KP, indicating that KP existed in the drug loading system in an amorphous state. In addition, the f-SWCNTs and f-SWCNTs-KP has a wide and indistinct diffraction peak at 24-28°, which may be related to the hexagonal graphite structure of SWCNTs (Xin et al. 2013). The results showed that the drug loading process did not affect the graphene microcrystal structure of carbon SWCNTs, which were

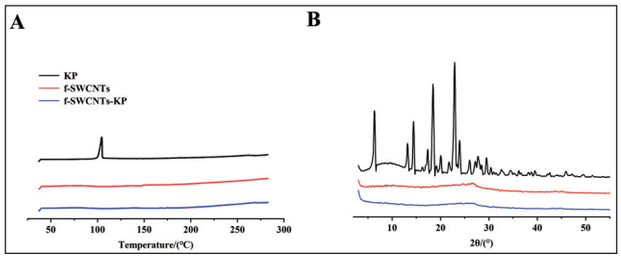

Fig. 3: (A) DSC patterns and (B) XRD patterns: (a) KP; (b) f-SWCNTs; (c) f-SWCNTs-KP

similar to the XRD results of biomolecule loaded nanotubes by Zheng et al (Xin et al. 2013).

The FTIR spectra of p-SWCNTs, f-SWCNTs, f-SWCNTs-KP and KP are shown in Fig. 4. In the FTIR spectra of the carbon nanotubes system, the -OH and C=O stretching vibrations of the p-SWCNTs led to the absorption peaks at 3433 and 1630 cm^{-1}, respectively. In the FTIR spectra of f-SWCNTs and f-SWCNTs-KP, there were -CH_2- characteristic peaks of PEI at 2918 and 2847 cm^{-1}, and characteristic peaks of amide II and III bands at 1520 cm^{-1} and 1311 cm^{-1}, and the results were similar to those of Guo et al. (2013), which further proved that PEI was covalently modified to the surface of CNTs-COOH by amide bond. In the FTIR spectra of f-SWCNTs-KP, it may due to the -OH on KP that obviously broadened the absorption peak at 3433 cm^{-1}, and showed the C-H stretching vibration absorption of KP at 1447.39 and 1386.54 cm^{-1}. These results indicated that KP was successfully loaded into f-SWCNTs.

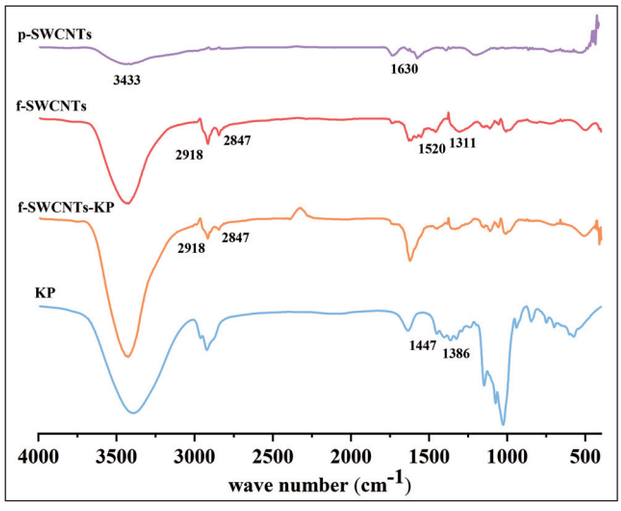

Fig. 4: FTIR spectrogram: (a): p-SWCNTs; (b): f-SWCNTs; (c): f-SWCNTs-KP; (d): KP

2.3. *In vitro drug release study*

The cumulative release of KP from the free drug KP, f-SWCNTs-KP and f-SWCNTs-KP-ES in the PBS buffer can be seen in Fig. 5A. The free drug KP was released quickly and completely during the first 4 h. When KP was loaded into f-SWCNTs, the release rates of KP were 71.15±1.57% at 4 h and 83.56±1.77% at 24 h, indicating delayed drug release. What's more, the release trend of f-SWCNTs-KP-ES was similar to that of f-SWCNTs-KP, but the release rate of KP in the first two hours was relatively slow, which may be due to the slow release of drug-loaded carbon nanotubes encapsulated by ethosomes. After two hours, the structure of some ethosomes may be destroyed in the PBS release system, with the ethanol solvent accelerating the release of KP in f-SWCNTs-KP-ES, making the later release rate similar to that of f-SWCNTs-KP. In addition, the release rates of f-SWCNTs-KP were faster in the first four hours, which may be the release stage of KP adsorbed into the surface of

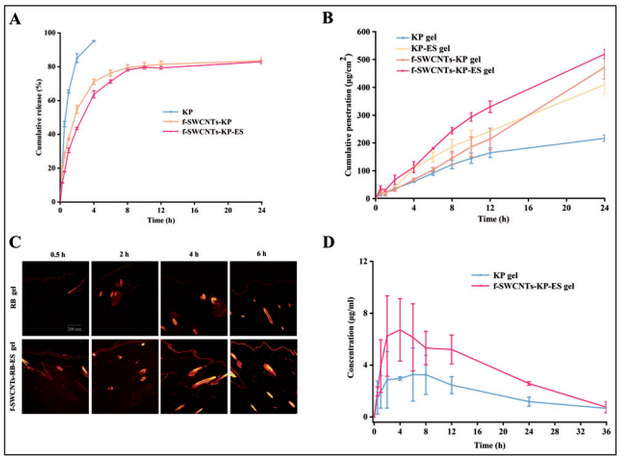

Fig. 5: (A) The cumulative release of KP of free drug KP, f-SWCNTs-KP and f-SWCNTs-KP-ES in PBS buffer, pH=7.4 (n=3); (B) Rat skin permeation profiles of KP gel, KP-ES gel, f-SWCNTs-KP gel and f-SWCNTs-KP-ES gel (n=6); (C) Fluorescence microscope images of longitudinal section of the skin of rat of rhodamine B labeled RB gel and f-SWCNTs- RB -ES gel; (D) The concentration-time curve of KP in rat plasma after transdermal administration of KP gel and f-SWCNTs-KP-ES gel (mean±SD, n=6)

SWCNTs. After four hours, the release rates of KP became slower, which may be the release stage of KP wrapped in the cavities of carbon nanotubes. Table 2 shows that the drug release behaviors of f-SWCNTs-KP and f-SWCNTs-KP-ES were in accordance with the first-order kinetic equation, and the regression equations were lnQ = 0.64725t + 4.3833 and lnQ = 0.41597t + 4.3881, R^2 were 0.9768 and 0.9919, respectively.

Table 2: Fitting equations of different drug release models

Drug delivery system	Model	Regression equation	R^2
f-SWCNTs-KP	zero-order kinetic	Q= 0.47522t+44.29891	0.4792
	first-order kinetic	lnQ=0.64725t+4.3833	0.9768
	Higuchi	Q= 15.69966t^1/2+25.86264	0.7551
	Ritger-Peppas	Q= 42.32716$t^{0.26209}$	0.8692
f-SWCNTs-KP-ES	zero-order kinetic	Q= 2.88875t+36.264	0.5351
	first-order kinetic	lnQ=0.41597t+4.3881	0.9919
	Higuchi	Q= 18.0001t^1/2+15.4707	0.8031
	Ritger-Peppas	Q= 35.0526$t^{0.32359}$	0.8774

2.4. *In vitro permeation study*

The cumulative penetration curves are shown in Fig. 5B. It was very intuitive that the cumulative penetration and transdermal rate of the f-SWCNTs-KP-ES gel were significantly improved. It can be seen from Table 3 that the permeation rates of different gels are as follows: f-SWCNTs-KP-ES gel > KP-ES gel > commercial gel > f-SWCNTs-KP gel > KP API gel. The mechanism of carbon nanotubes enhancing skin penetration is not clear. Although it has been reported that carbon nanotubes can be internalized by living cells and pass through the biofilm in the study of cell culture, it is found that carbon nanotubes cannot penetrate the skin and enter the body

Table 3: Skin permeation parameters of different KP formulations in vitro

Formulation	J_{ss} (μg/cm^2/h)	K_p (cm/h)	Q_{skin} (μg/cm^2)
KP gel	13.557±2.11	3.39×10^{-3}	10.54±1.77
KP-ES gel	21.993±3.04	5.50×10^{-3}	24.91±2.95
f-SWCNTs-KP gel	17.641±2.41	4.41×10^{-3}	19.79±0.94
f-SWCNTs-KP-ES gel	27.374±1.98	6.84×10^{-3}	31.79±2.16

Abbreviations: J_{ss}: steady-state fluxe; K_p: apparent permeability coefficient; Q_{skin}: the skin retention of per unit area

in this experiment, and the experimental results are consistent with literature data (Degim et al. 2010; Ilbasmis and Degim 2012). In addition, the enhanced penetration of drug-loaded carbon nanotubes may be achieved through adsorption and subsequent desorption (i.e. storage effect) (Degim et al. 2010; Ilbasmis and Degim 2012). The combination of KP and SWCNTs was relatively strong. Although SWCNTs significantly increased the solubility of KP, it was difficult to release KP and limited its transdermal absorption. On the other hand, the permeation rate of KP-ES gel was higher than that of f-SWCNTs-KP gel, which further indicated that ethosomes had a significant advantage in promoting drug penetration. The possible reason is the existence of ethanol, which is a well-known penetration enhancer (Zhang et al. 2012). Ethanol has the ability to disrupt the multi-layer ordered lipid domains, reduce the structural density and increase the fluidity of the stratum corneum, which will provide flexible properties for ethosome vesicles, allowing them to easily penetrate deeper skin layers (Abd et al. 2019; Bodade et al. 2013). Another important factor is the easy fusion of phospholipids between the ethosome vesicles and the stratum corneum, which changes the transition temperature and leads to the improvement of drug penetration (Yu et al. 2015). There were significant differences in skin retention between KP carbon nanotube gel group and KP-ES gel group and KP gel group, showing that both ethosomes and f-SWCNTs could increase drug retention and form drug storage. Therefore, it is necessary to make KP into a composite preparation and give full play to the advantages of ethosomes and f-SWCNTs at the same time, which will provide some new mentalities for the clinical application of KP and is of great significance to give better play to the clinical efficacy.

Fluorescence microscope images of longitudinal sections of the skin are shown in Fig. 5C. After permeation with RB gel and f-SWCNTs-RB-ES gel, fluorescence was first detected in the cuticle and the fluorescence distribution of each tissue layer in the skin increased with time. As the control group, RB gel showed the least fluorescence color at each time in the skin, which showed that its penetration ability was relatively poor. The fluorescence of f-SWCNTs-RB-ES gel group basically covered the whole stratum corneum, active epidermis and dermis four hours after treatment, and the fluorescence of the former group was stronger than that of the latter group, and the fluorescence distribution of the two groups did not increase significantly after six hours. The possible reason was that small ethosomes enhanced transdermal performance by altering the structure of the lipid layer in the skin (Celebi et al. 2015; Jain et al. 2014). This result was in accordance with that of permeation study, which further indicated that f-SWCNTs-RB-ES could significantly improve the penetration of drug through the stratum corneum and prolong the action time of the drug.

2.5. *In vivo studies*

The changes of plasma KP concentration with time in SD rats after application of KP gel and f-SWCNTs-KP-ES gel are shown in Fig. 5D, which are accorded with the two-compartment model. It can be seen that the absorption rate of f-SWCNTs-KP-ES gel group was faster than that of KP gel group, and the peak time T_{max} was 3.5 h. And the plasma KP concentration increased gradually at the initial stage of administration, and decreased gradually after absorption to a certain extent in f-SWCNTs-KP-ES gel group. In addition, the plasma KP concentration decreased more slowly in the later stage, and the sustained release effect was obvious.

The pharmacokinetic parameters of percutaneous administration were listed in Table 4. The $T_{1/2Ka}$ of f-SWCNTs-KP-ES gel group was 1.02±0.285 h ($P < 0.05$), indicating that the gel was absorbed quickly in rat skin. The peak concentration (C_{max}) of the f-SWCNTs-KP-ES gel group was 7.71±1.23 mg·L^{-1}, which was significantly 2.36 times higher than that of the KP gel group ($P < 0.05$), and the peak concentration lasted for a long time. In addition, the area under the drug time curve (AUC_{0-t}) of the f-SWCNTs-KP-ES gel group was 110.79±8.78 mg/L*h, which was 1.97 times higher than that of the KP gel group, indicating that the preparation could effectively improve the bioavailability of KP (Aqil et al. 2016). The $T_{1/2\beta}$ of f-SWCNTs-KP-ES gel group and drug retention time (MRT_{0-t}) was 25.41 ± 3.10 h and 10.25 ± 1.96 h, respectively, which were longer than those in KP gel group ($P < 0.05$), and the drug clearance rate (CL) was greatly reduced. The above results indicated that f-SWCNTs-KP-ES gel could prolong the residence time of KP in vivo and improve the efficacy of the drug to a certain extent.

Table 4: The pharmacokinetic parameters of percutaneous administration were analyzed according to the two-compartment model

parameter	unit	KP gel	F-SWCNTs-KP-ES gel
T_{max}	h	5.5±0.87	3.5±0.94
C_{max}	mg/L	3.27±0.48	7.71±1.23
CL	L/h	0.07±0.003	0.03±0.001
$T_{1/2\alpha}$	h	4.49±0.83	1.73±0.66
$T_{1/2\beta}$	h	18.81±1.17	25.41±3.10
$T_{1/2Ka}$	h	3.09±0.102	1.02±0.285
k_{10}	1/h	0.09±0.019	0.09±0.007
k_{12}	1/h	0.03±0.003	0.12±0.034
k_{21}	1/h	0.06±0.016	0.10±0.013
AUC_{0-t}	mg/L*h	56.10±3.50	110.79±8.78
$AUC_{0-\infty}$	mg/L*h	58.23±2.44	139.63±5.35
MRT_{0-t}	h	10.05±1.06	10.25±1.96

Note: *P<0.05, statistical significance compared to KP gel.
Abbreviations: T_{max}: peak time; C_{max}: peak concentration; CL: clearance; $T_{1/2\alpha}$: distribution half-life; $T_{1/2\beta}$: elimination half-life; k_{10}, k_{12}, and k_{21}: elimination rate constants; AUC: area of the curve of plasma concentration versus time; MRT: mean retention time

2.6. *Conclusions*

In this study, KP-loaded f-SWCNTs composite ethosomes (f-SWCNTs-KP-ES) were successfully prepared by a single-step injection technology and verified by a series of characterizations. After transdermal administration, compared with free gel, they can significantly enhance the skin permeation of KP and increase its bioavailability. Obviously, f-SWCNTs-KP-ES are a promising drug carrier with application prospect which has certain significance for the development of prospective drug system for transdermal delivery. The study design is summarized graphically in Fig. 6.

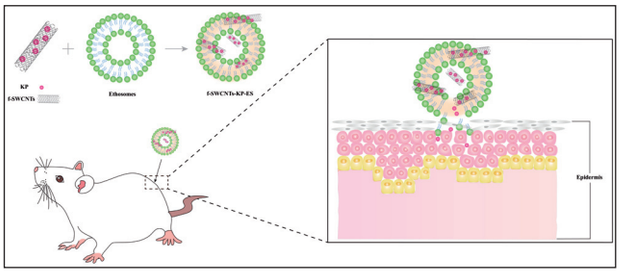

Fig. 6: Graphical summary of the study design

3. Experimental

3.1. *Materials*

SWCNTs were purchased from Chengdu Organic Chemicals Co. Ltd., Chinese Academy of Sciences (Chengdu, China). Concentrated nitric acid (HNO3) and concentrated sulfuric acid (H2SO4) were acquired from Guangzhou Chemical Reagent Factory (Guangzhou, China); KP (purity 98%), PEI (MW=10 KDa, purity > 99%), 1-ethyl-3-(3-(dimethylamino) propyl) carbodiimide hydrochloride (EDC) and N-hydroxysuccinimide (NHS) were obtained from Shanghai Aladdin Biochemical Technology Co., Ltd., (Shanghai, China); Cholesterol and egg yolk lecithin (PC-100M) were purchased from Shanghai AVT Pharmaceutical Co. Ltd., (Shanghai, China); Naproxen control (purity 99.5%) from China Institute for the Control of Pharmaceutical and Biological Products; Carbopol 940 from BASF (Germany). And other chemicals and reagents were of analytical grades.

3.2. *Preparation of f-SWCNTs-KP-ES*

The preparation process of f-SWCNTs-KP-ES is as follows: 500 mg pristine single-walled carbon nanotubes (p-SWCNTs) were put into a mixture of concentrated H_2SO_4 and HNO_3 (1: 3 v/v), mixed evenly with a glass rod and refluxed for 3 hours at 80 °C

(Abousalman-Rezvani et al. 2020). After cooling to room temperature, the reactants were diluted with distilled water and left overnight. The supernatant was poured out, and an appropriate amount of distilled water was added to neutralize the mixed acid. The filter cake was washed with distilled water to neutral after vacuum filtration with a Brinell funnel, and the product was dried to constant weight to obtain truncated carboxylated single-walled carbon nanotubes (SWCNTs-COOH) with a large number of carboxyl groups (Dlamini et al. 2019).

The prescribed amount of SWCNTs-COOH were ultrasonic for 20 min until they were completely dispersed in distilled water, and the dispersion was placed on a magnetic stirrer. 0.1 mmol EDC and 0.1 mmol NHS were slowly added to the dispersion to activate the carboxyl group, and then 50 mg of PEI aqueous solution was added. After 24 h of reaction, the mixture was loaded into a dialysis bag (MW=8-14 KDa). The dialysis bag was placed in distilled water (changing the water every 6 h) and the unreacted PEI and catalysts were removed by magnetic stirring for 48 h. And the f-SWCNTs black powder was obtained by freeze-drying (Nahid et al. 2014).

An appropriate amount of KP was precisely weighed and the volume was fixed with ethanol. The prescribed amount of f-SWCNTs was weighed and placed in the cillin bottle of 10 ml. An appropriate amount of ultrapure water was added to f-SWCNTs under probe ultrasound to make it disperse evenly, and a known content of KP ethanol solution was slowly injected into the aqueous dispersion of f-SWCNTs with a 1ml syringe (Yu et al. 2016). After a certain time, f-SWCNTs-KP was obtained by evaporating ethanol with a magnetic agitator at 50 °C.

F-SWCNTs-KP-ES were prepared by a single-step injection technique. Firstly, a mixture of ethanol and propylene glycol (3:1, v/v) was prepared to dissolve the prescribed amounts of egg yolk lecithin and cholesterol and stirred magnetically at 700 rpm for 5 min. Secondly, the previously prepared f-SWCNTs-KP aqueous dispersion was slowly injected into the ethanol lecithin solution with a 1 ml syringe (Pippa et al. 2017). Finally, after magnetic stirring for 10 min, f-SWCNTs-KP-ES were obtained under probe ultrasound (output power of 40%) for 10 min at 400 W.

3.3. Preparation of gel

In order to facilitate the later *in vitro* transdermal experiment and *in vivo* pharmacokinetic study, the prepared liquid preparation was made into gel. Carbomer 940 was used as gel matrix, and the liquid preparation was made into 1.0% hydrogel through pre-experimental investigation. In the experiment, the prescribed amount of Carbomer 940 was added to a beaker and the prepared liquid preparation was added to it to fully swell. And then triethanolamine was added drop by drop under continuous stirring until neutral to obtain gel. Besides, the fluorescent labeling preparation was prepared by using RB instead of the free drug KP. The RB concentration (0.02%) of RB-loaded f-SWCNTs-ES (f-SWCNTs-RB-ES) was the same as that of RB aqueous solution and were prepared into gels according to the above method.

3.4. Water dispersibility of carbon nanotubes

SWCNTs, SWCNTs-COOH and f-SWCNTs (5 mg) were dispersed in distilled water, respectively. After ultrasonic with a cell crushing apparatus for 10 min at 400 W, the dispersion was observed, and the aggregation of substances in the solution was recorded.

3.5. Characterization of SWCNTs system

The microscopic morphology of the samples was studied by transmission electron microscopy (TEM) (HT7700, Hitachi, Tokyo, Japan). The prepared sample was properly diluted with distilled water and a droplet of the sample suspension was placed onto a carbon-coated copper grid and the excess liquid was immediately absorbed with filter paper followed by drying naturally at room temperature. Then the sample was put onto the microscope and observed under the accelerated voltage of 80 kV, and the surface characteristics and shapes were evaluated at appropriate magnification (Abd et al. 2019).

KP-ES, f-SWCNTs, f-SWCNTs-KP and f-SWCNTs-KP-ES were diluted to appropriate concentration with distilled water, and the particle size of the samples were measured by a Delsa Nano C particle analyzer (Beckman Coulter Instruments, Brea, CA, USA). Then the zeta potential of the samples was measured. Each sample was measured in triplicate at 25±0.2 °C.

Approximately 5.0 mg of samples were weighed and put into an aluminum crucible, and DSC experiment was carried out. The sample was scanned in the range of 30–280 °C, using nitrogen as carrier gas, and the heating rate was 10 °C / min (Liu et al. 2018).

A X-ray single crystal diffractometer (Rigaku Corporation, Tokyo, Japan) was used to analyze the sample powder which was stacked into a square, compacted and placed in the sample tray. And the detection conditions are as follows: Cu target K α-ray, voltage 40 kV, a current of 40 mA, emission slit 1/32 °, anti-scattering slit 1/16 °, 2 θ range: 3 °- 55 °, step width 0.02 °, and residence time of each step is 40 s.

A Spectrum 100 FTIR Spectrometer (Perkin Elmer Corp., San Jose, California, USA) was used to obtain FTIR spectra of a series of samples related to SWCNTs. The trace dry solid sample was mixed with about 110 mg potassium bromide, ground into powder in a mortar and pressed into a thin sheet, and the Fourier transform infrared spectrum was scanned between 4000 and 400 cm^{-1} at a resolution of 1 cm^{-1}.

3.6. In vitro drug release study

KP suspension, f-SWCNTs-KP and f-SWCNTs-KP-ES (5 mL) were added to the dialysis bag (MW = 8-14 KDa) respectively, both ends were clamped and checked for leakage. The dialysis bags were then placed in 70 mL PBS (pH 7.4) with oscillation of 100 rpm at 37 °C, ensuring the liquid level was submerged over the dialysis bags. 2.5 mL solutions were collected at predetermined intervals, which were 1, 2, 4, 6, 8, 10, 12, and 24 h, and the same volume of fresh PBS solution was replenished (Ruiz et al. 2020). Afterwards, HPLC was used to determine the concentration of KP in each sample, and the cumulative release percentage at each time point was calculated, and the release curve was plotted. All the experiments were repeated three times. According to the *in vitro* drug release data of f-SWCNTs-KP, it is fitted into four kinetic models, namely, zero-order kinetic equation, first-order kinetic equation, Higuchi equation and Ritger-Peppas equation, so as to analyze the *in vitro* drug release characteristics of the preparation, and determine the most suitable kinetic model according to R^2.

3.7. In vitro skin permeation study

After SD rats, weighing 200±20 g, were anesthetized with phenobarbital sodium, the back hair of the rats was shaved with electric push scissors, and the excess hair was depilated with depilatory creams. The rats were sacrificed after 12 h of feeding and the back skin was separated by surgery. The subcutaneous fat and tissues of the rat's back skin were removed with scalpel and hemostatic forceps, and the full-thickness skin was washed with normal saline. After absorbing the excess moisture with filter paper, the full-thickness skin was wrapped with fresh-keeping film and stored at -20 °C. The skin was taken out before the experiment, and the skin integrity of rats was checked after natural thawing at room temperature.

In vitro permeation experiments were carried out in a Franz diffusion cell using the back skin of SD rats (Zhang et al. 2016). Firstly, the magnetic stirrer was put into the receiver chamber and the full-thickness skin was fixed between the donor and receiver chamber. The dermis was in contact with the drug supply layer, and each gel preparation was smeared to the dermis, in which the dosage of the KP gel group, KP-ES gel group and the f-SWCNTs-KP-ES gel group were 1 g (0.4% KP). After that, PBS (pH 7.4) was slowly injected into the receiver chamber equipped with a stir bar and acted as the diffusion medium. In order to avoid the influence of air bubbles in the receiver chamber on transdermal effect, the diffusion medium was degassed by ultrasonic in advance. What's more, the diffusion medium should be in close contact with the skin, and the top of the diffusion medium should be sealed with fresh-keeping film to prevent water evaporation. The receiver chamber placed in a constant temperature controlled shaking water bath was kept at 37±0.5 °C and continuously stirred with 100 rpm (Hussain et al. 2013). 2.5 mL receiving medium was removed from the receiver chamber at 0.5, 1, 2, 4, 6, 8, 10, 12 and 24 h, respectively, and the equal volume of diffusion medium was replenished (Xie et al. 2018). The skin of the rats administered with the drug was taken out after 24 h, the gel coated on the surface was scratched off and cleaned with distilled water, the excess moisture of the skin was absorbed with filter paper. After the skin was shredded, an appropriate amount of methanol was added for ultrasound for 15 min, centrifuged at 10,000 rpm for 5 min and filtered with a 0.22 μm microporous membrane. The amount of the drug penetration at each time point was analyzed by HPLC, and according to the following equation the cumulative amount of drugs penetration through the skin per unit area (Q_n), apparent permeability coefficient (K_p) and the amount of retention per unit area of the skin (Q_{skin}) were calculated, respectively:

$$Q_n(\%) = \frac{C_n V_r + \sum_{i=1}^{n-1} C_i V_s}{A} \quad (1)$$

Where Q_n is the cumulative amount of drugs penetration through the skin per unit area, C_n is the drug concentration of the receiver solution KP at each test time t, and V_r is the volume of the receiving cell, and C_i is the KP concentration of the receiver solution at the previous time point of each test time t, and V_s is the volume of sampled receiving liquid, and A is the effective penetration area of the diffusion cell.

$$K_p = \frac{Jss}{C_0} \quad (2)$$

Where K_p is the apparent permeability coefficient, J_{ss} is the slope of the cumulative permeation amount curve, and C_0 is the concentration of the test product in the donor compartment.

$$Q_{skin} = \frac{CV}{A} \quad (3)$$

Where the Q_{skin} is the amount of retention per unit area of the skin, C is the concentration of KP in the methanol extract of the skin, and V is the volume of the methanol extract of the skin.

3.8. Fluorescence microscopy

According to the above method, the fluorescent labeling preparation RB gel and f-SWCNTs-RB-ES gel were administered to the back skin of SD rats to study *in vitro* skin permeation. The skin tissues were removed at 0.5, 1, 2 and 6 h after administration and the residual fluorescent RB on the surface of the skin was wiped clean by cotton balls. The rat skin permeated by RB gel and f-SWCNTs-RB-ES gel was solidified and dehydrated respectively. The skin was placed flat in a jar containing 4% paraformaldehyde solution, solidified overnight, rinsed with distilled water, soaked in 20% sucrose for 12 h and the water was wiped away with filter paper. The treated skin was cut into 1×1 cm^2 pieces with surgical scissors and the optimal cutting temperature compound (O.C.T) was added at -20 °C and then the skin was horizontally fixed. Then the skin was longitudinally sliced by using a cryostat microtome (CM1860, Leica Instruments) to obtain longitudinal sections with a thickness of 10 μm. The sections were placed on glass slides and sealed with anhydrous glycerin (Lin et al. 2018; Xie et al. 2018). The sections were investigated for RB distribution under a fluorescence microscope (CKX311, Olympus Corp., Tokyo, Japan). The RB color channel of fluorescence microscope was opened, the excitation/emission wavelength was 554 nm/575 nm, and the emission fluorescence was red light.

3.9. In vivo pharmacokinetic studies

Time-sharing sampling for *in vivo* administration was adopted (Wei et al. 2012). Male SD rats were used to compare the pharmacokinetics of KP gel and f-SWCNTs-KP-ES gel after transdermal administration, so as to provide basis for clinical application. Tvelve male SD rats weighing 200±20 g were randomly divided into two groups, the hair on the neck and back of the rats was shaved off, and the rats were fasted for 12 h but could drink water freely before the experiment. Phenobarbital sodium (2%, 50 mg/kg) was injected into the abdominal cavity of rats. After the rats were anesthetized, the gel was applied to the depilated back of the rats, in which the dosage of the KP gel group and the f-SWCNTs-KP-ES gel group were 1 g (0.4% KP). The administration area of 12 cm^2 (3×4 cm) was determined by marker on the back of rats, and then fixed with surgical patch and medical tape. Whole blood was collected through the orbital vein of rats for 0.5 mL at the time of 0. 5, 1, 2, 4, 6, 8, 12, 24, 36 h, respectively. The whole blood collected was put into the 1.5 mL EP tube and rinsed with heparin to avoid coagulation. The EP tube was centrifuged at 4000 rpm for 10 min and the upper liquid was separated to obtain plasma.

3.10. HPLC analysis of KP content in plasma

Plasma (200 µL) was added into tubes and 20 µL of naproxen internal standard solution (40 µg/ml) was precisely added. And then 100 µL of methanol and 600 µL of acetonitrile were mixed together in tubes for extraction (Porazka et al. 2017). The tubes were vortexed for 3 min and centrifuged at 8000 rpm for 10 min. After centrifugation, the supernatant was collected and dried under 50 °C nitrogen flow. After 200 µL mobile phase was added, the residue was redissolved, vortexed for 3 min and centrifuged at 10000 rpm for 10 min. The supernatant was sucked up and placed in the injection bottle for later use (Cheng et al. 2019).
Pharmacokinetic parameters were calculated by the pharmacokinetic software, DAS 2.0 (Drug and Statistics 2.0; the Committee of the Mathematic Pharmacology, the Chinese Society of Pharmacology, Hefei, China).

3.11. Statistical analysis

The GraphPad Prism 5.0 (GraphPad Software, Inc., San Diego, California) was used to analyze statistical and the results were expressed as mean±SD. And $P < 0.05$ was considered to indicate statistical significance.

Acknowledgments: This work was financially supported by the Guangzhou Science and Technology Plan Project (number 201904010112).

Ethical approval: All procedures performed involving animals were approved by the Animal Research Ethics Committee, Guangdong Pharmaceutical University.

Conflicts of Interests: No potential conflict of interest was reported by the author(s).

References

Abd El-Alim SH, Kassem AA, Basha M, Salama A (2019) Comparative study of liposomes, ethosomes and transfersomes as carriers for enhancing the transdermal delivery of diflunisal: In vitro and in vivo evaluation. Int J Pharm 563: 293-303.

Abousalman-Rezvani Z, Eskandari P, Roghani-Mamaqani H, Salami-Kalajahi M (2020) Functionalization of carbon nanotubes by combination of controlled radical polymerization and "grafting to" method. Adv Colloid Interface Sci 278: 102126.

Aqil M, Kamran M, Ahad A, Imam SS (2016) Development of clove oil based nanoemulsion of olmesartan for transdermal delivery: Box-Behnken design optimization and pharmacokinetic evaluation. J Mol Liq 214: 238-248.

Bodade SS, Shaikh KS, Kamble MS, Chaudhari PD (2013) A study on ethosomes as mode for transdermal delivery of an antidiabetic drug. Drug Deliv 20: 40-46.

Çelebi N, Ermiş S, Özkan S (2015) Development of topical hydrogels of terbinafine hydrochloride and evaluation of their antifungal activity. Drug Dev Ind Pharm 41: 631-639.

Dantas de Freitas E, Pires Rosa PC, Carlos da Silva MG, Adeodato Vieira MG (2018) Development of sericin/alginate beads of ketoprofen using experimental design: Formulation and in vitro dissolution evaluation. Powder Technol 335: 315-326.

Degim IT, Burgess DJ, Papadimitrakopoulos F (2010) Carbon nanotubes for transdermal drug delivery. J Microencapsul 27: 669-681.

Dinan NM, Atyabi F, Rouini MR, Amini M, Golabchifar AA, Dinarvand R (2014) Doxorubicin loaded folate-targeted carbon nanotubes: preparation, cellular internalization, in vitro cytotoxicity and disposition kinetic study in the isolated perfused rat liver. Mater Sci Eng C Mater Biol Appl 39: 47-55.

Dlamini N, Mukaya HE, Van Zyl RL, Chen CT, Zeevaart RJ, Mbianda XY (2019) Synthesis, characterization, kinetic drug release and anticancer activity of bisphosphonates multi-walled carbon nanotube conjugates. Mater Sci Eng C Mater Biol Appl 104: 109967.

Farahani BV, Behbahani GR, Javadi N (2015) Functionalized multi walled carbon nanotubes as a carrier for doxorubicin: drug adsorption study and statistical Optimization of drug loading by factorial design methodology. J Braz Chem Soc 27: 694-705.

Guo YK, Ren QX, Xiong Q, Sun L, Li XJ (2013) Preparation of multi-walled carbon nanotubes-polyethyleneimine composite and its cytotoxicity on PC12 cells. Chin Pharm J 48: 1558-1563.

He H, Pham-Huy LA, Dramou P, Xiao D, Zuo P, Pham-Huy C (2013) Carbon nanotubes: applications in pharmacy and medicine. Biomed Res Int 578290.

Hegde AR, Rewatkar PV, Manikkath J, Tupally K, Parekh HS, Mutalik S (2017) Peptide dendrimer-conjugates of ketoprofen: Synthesis and ex vivo and in vivo evaluations of passive diffusion, sonophoresis and iontophoresis for skin delivery. Eur J Pharm Sci 102: 237-249.

Hussain G, Kohli K, Umar A, Amin S (2013) Nanovesicular delivery of repaglinide through skin. Sci Adv Mater 5: 810-821.

Ilbasmis-Tamer S, Degim IT (2012) A feasible way to use carbon nanotubes to deliver drug molecules: transdermal application. Expert Opin Drug Deliv 9: 991-999.

Jain S, Patel N, Madan P, Lin S (2015) Quality by design approach for formulation, evaluation and statistical optimization of diclofenac-loaded ethosomes via transdermal route. Pharm Dev Technol 20: 473-489.

Jyothsna M, Aparna M, Gopal VS, Krishnamurthy B, Srinivas M (2017) Low frequency ultrasound and PAMAM dendrimer facilitated transdermal delivery of ketoprofen. J Drug Deliv Sci Technol 334-343.

Kaleemullah M, Jiyauddin K, Thiban E, Rasha S, Al-Dhalli S, Budiasih S, Gamal OE, Fadli A, Eddy Y (2017) Development and evaluation of ketoprofen sustained release matrix tablet using Hibiscus rosa-sinensis leaves mucilage. Saudi Pharm J 25: 770-779.

Kurniawan A, Muneekaew S, Hung CW, Chou SH, Wang MJ (2019) Modulated transdermal delivery of nonsteroidal anti-inflammatory drug by macroporous poly(vinyl alcohol)-graphene oxide nanocomposite films. Int J Pharm 566: 708-716.

Lin H, Xie Q, Huang X, Ban J, Wang B, Wei X, Chen Y, Lu Z (2018) Increased skin permeation efficiency of imperatorin via charged ultradeformable lipid vesicles for transdermal delivery. Int J Nanomedicine 13: 831-842.

Liu JJ, Cheng Y, Shao YY, Chang ZP, Guo YT, Feng XJ, Xu D, Zhang JP, Song Y, Hou RG (2019) Comparative pharmacokinetics and metabolites study of seven major bioactive components of Shaoyao-Gancao decoction in normal and polycystic ovary syndrome rats by ultra high pressure liquid chromatography with tandem mass spectrometry. J Sep Sci 42: 2534-2549.

Liu XH, Xu DQ, Lioa CC, Fang YQ, Guo BH (2018) Development of promising drug delivery for formononetin: cyclodextrin-modified single-walled carbon nanotubes. J Drug Deliv Sci Tec. 2018, 43: 461-468.

Malinovskaja-Gomez K, Espuelas S, Garrido MJ, Hirvonen J, Laaksonen T (2017) Comparison of liposomal drug formulations for transdermal iontophoretic drug delivery. Eur J Pharm Sci 106: 294-301.

Manikkath J, Hegde AR, Kalthur G, Parekh HS, Mutalik S (2017) Influence of peptide dendrimers and sonophoresis on the transdermal delivery of ketoprofen. Int J Pharm 521: 110-119.

Mishra NS, Kuila A, Nawaz A, Pichiah S, Leong KH, Jang M (2018) Engineered carbon nanotubes: review on the role of surface chemistry, mechanistic features, and toxicology in the adsorptive removal of aquatic pollutants. ChemistrySelect 3: 1040-1055.

Miyako E, Kono K, Yuba E, Hosokawa C, Nagai H, Hagihara Y (2012) Carbon nanotube-liposome supramolecular nanotrains for intelligent molecular-transport systems. Nat Commun 3: 1226.

Paolino D, Lucania G, Mardente D, Alhaique F, Fresta M (2005) Ethosomes for skin delivery of ammonium glycyrrhizinate: in vitro percutaneous permeation through human skin and in vivo anti-inflammatory activity on human volunteers. J Control Release 106: 99-110.

Perpétuo GL, Chierice GO, Ferreira LT, Fraga-Silva TFC, Venturini J, Arruda MSP, Bannach G, Castro RAE (2017) A combined approach using differential scanning calorimetry with polarized light thermomicroscopy in the investigation of ketoprofen and nicotinamide cocrystal. Thermochim Acta 651: 1-10.

Pippa N, Chronopoulos DD, Stellas D, Fernandez-Pacheco R, Arenal R, Demetzos C, Tagmatarchis N (2017) Design and development of multi-walled carbon nanotube-liposome drug delivery platforms. Int J Pharm 528: 429-439.

Porażka J, Karbownik A, Murawa D, Spychala A, Firlej M, Grabowski T, Murawa P, Grzeskowiak E, Szalek E (2017) The pharmacokinetics of oral ketoprofen in patients after gastric resection. Pharmacol Rep 69: 296-299.

Rattanapak T, Young K, Rades T, Hook S (2012) Comparative study of liposomes, transfersomes, ethosomes and cubosomes for transcutaneous immunisation: characterisation and in vitro skin penetration. J Pharm Pharmacol 64: 1560-1569.

Ruiz A, Ma G, Seitsonen J, Pereira SGT, Ruokolainen J, Al-Jamal WT (2020) Encapsulated doxorubicin crystals influence lysolipid temperature-sensitive liposomes release and therapeutic efficacy in vitro and in vivo. J Control Release 328: 665-678.

Wei J, Ma PC, Cao YP, Tao l, Li LJ (2012) Dermatopharmacokinetic study of 2 kinds of imiquimod creams in nude mice by using time-share sampling method in vivo. China Pharmacy 23: 3488-3490.

Xie J, Ji Y, Xue W, Ma D, Hu Y (2018) Hyaluronic acid-containing ethosomes as a potential carrier for transdermal drug delivery. Colloids Surf B Biointerfaces 172: 323-329.

Xing WS, Lu F (2018) Progress of ketoprofen in pharmaceutical research. Chinese J Rational Drug Use 15: 76-80.

Yu B, Tan L, Zheng R, Tan H, Zheng L (2016) Targeted delivery and controlled release of Paclitaxel for the treatment of lung cancer using single-walled carbon nanotubes. Mater Sci Eng C Mater Biol Appl 68: 579-584.

Yu X, Du L, Li Y, Fu G, Jin Y (2015) Improved anti-melanoma effect of a transdermal mitoxantrone ethosome gel. Biomed Pharmacother 73: 6-11.

Zhang JP, Wei YH, Zhou Y, Li YQ, Wu XA (2012) Ethosomes, binary ethosomes and transfersomes of terbinafine hydrochloride: a comparative study. Arch Pharm Res 35: 109-117.

Zhang L, Wang J, Chi H, Wang S (2016) Local anesthetic lidocaine delivery system: chitosan and hyaluronic acid-modified layer-by-layer lipid nanoparticles. Drug Deliv 23: 3529-3537.

Zheng X, Wang TY, Jiang HT, Li YT, Jiang TY, Zhang JH, Wang SL (2013) Incorporation of carvedilol into PAMAM-functionalized MWNTs as a sustained drug delivery system for enhanced dissolution and drug-loading capacity. Asian J Pharm Sci 8: 278-286.

Zhu XL, Xie YX, Zhang YJ, Huang HQ, Huang SN, Hou L, Zhang HJ, Li Z, Shi JJ, Zhang ZZ (2014) Thermo-sensitive liposomes loaded with doxorubicin and lysine modified single-walled carbon nanotubes as tumor-targeting drug delivery system. J Biomater Appl 29: 769-779.